Fort Hays State University

FHSU Scholars Repository

Human umbilical cord blood mesenchymal stem cells engineered to overexpress growth factors accelerate outcomes in hair growth

Dong Ho Bak
Chung-Ang University

Mi Ji Choi
Chung-Ang University

Soon Re Kim
Chung-Ang University

Byung Chul Lee
Chung-Ang University

Jae Min Kim
Chung-Ang University

See next page for additional authors

Recommended Citation

Bak, D. H., Choi, M. J., Kim, S. R., Lee, B. C., Kim, J. M., Jeon, E. S., Oh, W., Lim, E. S., Park, B. C., Kim, M. J., Na, J., & Kim, B. J. (2018). Human umbilical cord blood mesenchymal stem cells engineered to overexpress growth factors accelerate outcomes in hair growth. The Korean Journal of Physiology & Pharmacology, 22(5), 555–566. https://doi.org/10.4196/kjpp.2018.22.5.555

Authors

Dong Ho Bak, Mi Ji Choi, Soon Re Kim, Byung Chul Lee, Jae Min Kim, Eun Su Jeon, Wonil Oh, Ee Seok Lim, Byung Cheol Park, Moo Joong Kim, Jungtae Na, and Beom Joon Kim

KJPP

Original Article

Human umbilical cord blood mesenchymal stem cells engineered to overexpress growth factors accelerate outcomes in hair growth

Dong Ho Bak[1,2,#], Mi Ji Choi[1,2,#], Soon Re Kim[1], Byung Chul Lee[1], Jae Min Kim[2], Eun Su Jeon[3], Wonil Oh[3], Ee Seok Lim[4], Byung Cheol Park[5], Moo Joong Kim[6], Jungtae Na[1,*], and Beom Joon Kim[1,2,*]

[1]Department of Dermatology, College of Medicine, Chung-Ang University, Seoul 06973, Korea, [2]Department of Medicine, Graduate School, Chung-Ang University, Seoul 06973, Korea, [3]Biomedical Research Institute, R&D Center, MEDIPOST Co., Ltd., Seongnam 13494, Korea, [4]Thema Dermatologic Clinic, Seoul 06524, Korea, [5]Department of Dermatology, Dankook Medical College, Cheonan 31116, Korea, [6]Fort Hays State University, Hays, KS 67601, USA

ABSTRACT Human umbilical cord blood mesenchymal stem cells (hUCB-MSCs) are used in tissue repair and regeneration; however, the mechanisms involved are not well understood. We investigated the hair growth-promoting effects of hUCB-MSCs treatment to determine whether hUCB-MSCs enhance the promotion of hair growth. Furthermore, we attempted to identify the factors responsible for hair growth. The effects of hUCB-MSCs on hair growth were investigated *in vivo*, and hUCB-MSCs advanced anagen onset and hair follicle neogeneration. We found that hUCB-MSCs co-culture increased the viability and up-regulated hair induction-related proteins of human dermal papilla cells (hDPCs) *in vitro*. A growth factor antibody array revealed that secretory factors from hUCB-MSCs are related to hair growth. Insulin-like growth factor binding protein-1 (IGFBP-1) and vascular endothelial growth factor (VEGF) were increased in co-culture medium. Finally, we found that IGFBP-1, through the co-localization of an IGF-1 and IGFBP-1, had positive effects on cell viability; VEGF secretion; expression of alkaline phosphatase (ALP), CD133, and β-catenin; and formation of hDPCs 3D spheroids. Taken together, these data suggest that hUCB-MSCs promote hair growth via a paracrine mechanism.

INTRODUCTION

Alopecia (hair loss) occurs due to many internal factors, such as aging or hormonal balance disruption, as well as diverse diseases and serious burns or wounds [1,2]. Hair loss is commonly accompanied by a region of thinned skin at the bald site [3,4]. Furthermore, these symptoms are due to the functional loss of follicular stem cell activity (i.e., forming the hair follicles) [5]. Recently, there have been numerous therapeutic trials of various treatments for hair loss such as oral medications and hair transplantation [6,7]. However, therapeutic drugs, like finasteride and dutasteride,

provide only temporary improvement, and often with reduced effectiveness, which results in immediate hair loss [8-10]. Although hair transplantation can replace the bald area with healthy hair, it is an invasive surgery, and a sufficient number of hairs for replacement is not always available in patients with severe hair loss [11]. Therefore, alternative therapeutic strategies are essential for alopecia.

The hair follicle (HF) cycle includes the phases of growth (anagen), regression (catagen), and rest (telogen) [12]. The activity of HFs can be influenced by the internal and external environments [13]. The mature HF has a complex structure with multilayered,

concentric epithelial basement cylinders of keratinocytes and a distinctive mesenchyme of human dermal papilla cells (hDPCs) [14]. hDPCs are the main component of HFs and are widely studied as the key functional center responsible for controlling the hair cycle throughout an animal's life cycle [15]. The androgen activators dihydrotestosterone and dickkopf-1, which can initiate damage-induced apoptosis of hDPCs, are some of the many factors involved in androgenic alopecia, where the HF cycle is incrementally arrested during the telogen phase and in which scalp hair follicles are gradually replaced by smaller follicles [16,17]. Thus, hDPCs may play a pivotal role in the pathogenesis of alopecia.

Human umbilical cord blood-derived mesenchymal stem cells (hUCB-MSCs) have been suggested to promote tissue repair and have been used for tissue engineering in numerous studies [18,19]. Not only can their multiple lineages replace aged or damaged cells, but their secretory factors can enhance tissue repair efficiency [20]. Human mesenchymal stem cells (hMSCs), which are capable of self-renewal and differentiation into various mesenchymal tissues, including osteogenic, adipogenic, and chondrogenic cell lineages, have been recognized as a promising tool for clinical applications [21]. However, the secretion of soluble factors is one of the key mechanisms underlying the therapeutic potential of hUCB-MSCs recently shown to have therapeutic efficacy in various disease models [22,23]. Transplantation of *ex vivo*-expanded hUCB-MSCs improved peripheral neuropathic pain [24] and focal cerebral ischemia [25] in rats. Thus, the treatment model of hUCB-MSC transplantation has been intensively studied for currently-untreated tissue impairments [26].

Hair loss from an adult follicle is considered to be a permanent state [27,28]. However, there are many therapeutic approaches to overcome this irreversible outcome [29]. A previous study has demonstrated that HF neo-genesis can be induced in wounds in mice in an mIGF-1-dependent manner [30]. On other hand, hair follicle stem cell differentiation is disturbed via inhibition of Wnt/b-catenin [31]. The IGF-1/AKT/GSK3β/β-catenin signaling pathway is crucial for cell protection and tissue regeneration [32,33]. The use of IGF-1/AKT/GSK3β/β-catenin on hDPCs in hair regeneration is groundbreaking. In this study, we used hUCB-MSCs to determine the effects of both stem cells and their paracrine factors on reacquisition of hDPC conduction ability to induce hair growth and to provide an effective therapeutic strategy for alopecia.

METHODS

Animals

C3H/HeJ mice were obtained from Saeron Bio Inc. (Gyeonggi-do, Korea) and allowed to adapt for one week with free access to food and water. The telogen-anagen transition model was in-duced by depilating the dorsal skin of mice in the telogen phase of the hair cycle, as described previously [34]. Starting one day after hair removal, minoxidill (3% v/w; Sigma-Aldrich; Merck KGaA, Darmstadt, Germany) was topically applied to the minoxidill group (MNX) for five days per week. At one day after hair removal, 400 μl of saline or hUCB-MSCs ($1×10^5$ cells/mice) were intradermally injected into multiple points (8 sites) in the skin of the injection control and hUCB-MSC groups, respectively. The dorsal skin was harvested for histological analysis at the end of the observation period (six weeks). The skin was then fixed in 4% formaldehyde and processed by paraffin block embedding using standard techniques to produce paraffin sections (10 μm thick). The general histology was visualized using hematoxylin-eosin (HE) staining. Immunohistochemistry was performed on sections that had been steamed in 10 mM sodium citrate (pH 6.0, cat. no. 005000, Fisher Scientific, Inc., Waltham, MA, USA) for 15 min prior to incubation with primary antibody. We used antibodies directed against β-catenin (1:500, cat. no. 610153, BD Biosciences, Franklin Lakes, NJ, USA). Primary antibodies were detected by biotinylated secondary antibodies plus streptavidin-peroxidase complex (cat. no. SA-5004, VECTOR LABORATORIES, INC., Burlingame, CA, USA) and brown FAST DAB staining (cat. no. 34002, Thermo Fisher Scientific, Inc., Waltham, MA, USA). Counterstaining of sections was performed using hematoxylin for DAB-stained sections light microscopy (DM750, Leica, Wetzlar, Germany). The protocol was approved by the medical ethics committee of Chung-Ang University (Seoul, Korea).

Isolation and culture of hDPCs

hDPCs were purchased from Cefobio (Seoul, Korea) as primary cells and were grown in Dulbecco's modified Eagle's medium (DMEM; Invitrogen/Gibco-BRL, Grand Island, NY, USA) supplemented with 5% fetal bovine serum (FBS; Invitrogen/Gibco-BRL) and 1% penicillin in a humidified environment. hDPCs in the third or fourth passage were used.

Patch assay

The hair-inductive capacity of the hDPCs was assessed in accordance with the established patch assay [35]. Implantation was performed as described previously [36]. Briefly, hUCB-MSCs (U) were combined with freshly isolated neonatal mouse epidermal (K) and dermal cells (D) and co-transplanted subcutaneously into the skin on the backs of nude mice. The normal group, K plus D group, K plus U, and K plus D plus U group were injected on the same day. Two weeks later, skin samples were dissected from the mice and examined to verify hair induction.

Culture of hUCB-MSCs

This study was approved by the Institutional Review Board of

MEDIPOST Co., Ltd. Neonatal hUCB-MSCs were collected from umbilical veins. Mononuclear cells were isolated from hUCB by centrifugation on a Ficoll-Hypaque gradient (density: 1.077 g/cm^3; Sigma-Aldrich). The cells were then seeded at 5×10^5 cells/cm^2 in culture flasks. After colonies of spindle-shaped cells formed, the cells were reseeded for expansion. hUCB-MSCs were cultured in αMEM medium (Gibco; Thermo Fisher Scientific, Inc., Waltham, MA, USA) supplemented with 10% FBS (Gibco) and gentamycin (Gibco) in a humidified atmosphere containing 5% CO_2 and 3% O_2 at 37°C. Cells were passaged when they reached 80% confluency and either used for experiments or redistributed to new culture plates. In all experiments, hUCB-MSCs used were at passage 6.

Human dermal papilla cell isolation and co-culture with hUCB-MSCs

For co-culture experiments, 1×10^5 hDPCs were seeded into the lower chamber of a 6-well transwell plate (Corning, New York, NY, USA) containing co-culture medium (DMEM or MEM). Immediately after the dermal papilla cells attached, the medium was changed, and 2×10^5 hUCB-MSCs were placed into the upper chamber. The plates were incubated at 37°C with 5% CO_2 for the indicated times before each analysis.

Cell proliferation assay

hDPCs were plated at a density of 1×10^5 cells/well in 6-well plates and were continuously cultured for 120 h under each test condition. At days 2 and 5 of co-culture with hUCB-MSCs, the proliferation was measured using a WST-8 assay (Dojindo; Rockville, MD, USA). WST-8 solution (100 μL) was added to the cells in 1 ml incomplete DMEM and incubated for 1 h at 37°C. The absorbance was then measured at 450 nm using a SpectraMax 190 microplate reader (Molecular Devices, Sunnyvale, CA, USA).

Alkaline phosphatase (ALP) activity

hDPCs were seeded at a density of 1×10^5 cells/mL in 6-well plates. At days 2 and 5 of co-culture with hUCB-MSCs, ALP activity of the hDPCs was determined enzymologically using an ALP assay. After washing with 1X PBS, the cells were incubated in 0.1 M $NaNO_3$-Na_2CO_3 (Sigma-Aldrich) buffer containing 1% (v/v) Triton X-100 (Sigma-Aldrich) and 2 mM $MgSO_4$ (Sigma-Aldrich). Subsequently, 6 mM p-nitrophenyl phosphate (Sigma-Aldrich) was added as a substrate to each well and incubated for 30 minutes at 37°C. Finally, 1.5 M NaOH (Sigma-Aldrich) was added to stop the enzyme-substrate reaction. Optical density (OD) readings were performed at a wavelength of 405 nm using a SpectraMax 190 microplate reader (Molecular Devices, Sunnyvale, CA, USA).

Human growth factor and cytokine antibody array

The Raybio® Human Cytokine/Growth Factor Antibody array I (RayBiotech, Norcross, GA, USA) was used to assay 23 cytokines and 41 growth factors in the supernatants of the cell cultures. The array membranes were incubated in blocking buffer for 30 min at room temperature (RT), then 1 ml of conditioned medium from either the hDPC, hUCB-MSCs, or hDPC plus hUCB-MSCs group was added per well, followed by incubation for 1 h at RT. The membranes were washed five times in wash buffer at RT, a biotin-conjugated antibody was added, and the membranes were incubated for 1–2 h at RT. The membranes were washed again, 2 ml of HRP-conjugated streptavidin was added, and the membranes were incubated for 2 h. Following incubation with detection buffer for 2 min, the luminescence was detected using the LAS 3000 chemiluminescence imaging system (Fujifilm Inc., Tokyo, Japan) and analyzed by densitometry using ImageJ 1.44 software (National Institutes of Health, Bethesda, MD, USA).

ELISA

The levels of insulin-like growth factor-1 (cat. no. DG100, R&D Systems, Minneapolis, MN, USA), insulin-like growth factor binding protein-1 (cat. no. DGB100, R&D Systems), and vascular endothelial growth factor (cat. no. DVE00, R&D Systems) in cell culture supernatants were quantified using an immunoassay kit. After each experiment, the collected medium was added to each well and incubated at room temperature for 2 h. The protein expression level was determined according to the manufacturer's protocol, and absorbance was measured at 450 nm using a SpectraMax 190 microplate reader (Molecular Devices).

Western blot analysis

Western blotting was performed as previously described using total protein obtained from hDPCs. Antibodies for phosphorylated-AKT (1:1000, cat. no. #9271, Cell Signaling Technology, Inc., Danvers, MA, USA), AKT (1:1000, cat. no. #4685, Cell Signaling Technology, Inc.), phopholyrated-GSK3β (1:1000, cat. no. #9323, Cell Signaling Technology, Inc), GSK3β (1:1000, cat. no. #12456, Cell Signaling Technology, Inc.), β-catenin (1:1000, cat. no. 610153, BD Biosciences, Franklin Lakes, NJ, USA), proliferating cell nuclear antigen (1:1000, cat. no. #13110, Cell Signaling Technology, Inc.), β-actin (1:1000, cat. no. sc-4778, Santa Cruz Biotechnology, Inc., Dallas, TX, USA), ALP (1:100, cat. no. SC-15065, Santa Cruz), CD 133 (cat. no. NB120-16518, Novus Biologicals, CO, USA) were used as the primary antibodies, and goat anti-rabbit (cat. no. BA-1000, VECTOR LABORATORIES, INC.) and goat anti-mouse (HRP) (cat. no. BA-9200, VECTOR LABORATORIES, INC.) were used as the secondary antibodies (1:10000). The blots were analyzed using densitometry with ImageJ 1.44 software (National Institutes of Health).

Establishment of hDPC micro-tissues in 3D hanging drop cultures

For 3D cell cultures, Perfecta3D Hanging Drop Plates (3D Biomatrix Inc., Ann Arbor, MI, USA) were used according to the manufacturer's protocol. To test the effects of IGFBP-1 on hD-PCs micro-tissue formation, the rhIGFBP-1 (cat. no. 871-B1-025, R&D Systems) (+) group was treated with rhIGFBP-1 (100 ng/ml). The size distribution of the resulting hDPCs micro tissues was analyzed to determine the optimal culture conditions. All hD-PCs were cultured in serum-free medium (DMEM), which was changed every 2 days using a multichannel pipette. The morphology and diameter of the hDPC spheroids were recorded using a reverse phase-contrast microscope (IX61 FL, Olympus Japan Co.) for up to 5 days.

Immunofluorescence staining

Immunofluorescence staining in hDPCs was performed as previously described [37]. Briefly, hDPCs were treated with rhIGFBP-1 (100 ng/ml) for 2 days. The cells were fixed in 10% neutral buffered formalin solution at room temperature for 30 minutes, permeabilized in 2.5% Tween 20 (cat. no. 9005-64-5, Sigma-Aldrich) in PBS for 5 min, then incubated overnight at 4°C with anti-ALP (1:500, cat. no. SC-15065, Santa Cruz), anti-β-catenin (1:500, cat. no. BD610154, BD Biosciences), anti-CD 133 (cat. no. NB120-16518, Novus Biologicals, CO, USA), anti-IGF-1 (cat. no. SC-9013 Santa Cruz), or anti-IGFBP-1 (cat. no. sc25257, Santa Cruz) primary antibody in blocking solution (1:1000). After several washes with PBS containing 0.5% Triton X-100 and 0.5% BSA, the hDPCs were incubated with anti-rabbit Cy2 (cat. no. 711-225-152, Jackson ImmunoResearch Inc., PA, USA) or anti–mouse (cat. no. 715-165-150; Jackson ImmunoResearch Inc.) labeled secondary antibodies for 1 h at RT. Following nuclear staining with DAPI dye (Sigma-Aldrich), the fluorescence signals were viewed using a Zeiss confocal laser microscope (LSM 700; Zeiss, Heidelberg, Germany).

Statistical analysis

Significant differences were determined using Student's t-test, with p<0.05 considered to be statistically significant. All data are presented as the mean±SEM.

RESULTS

hUCB-MSCs promote hair follicle cycling, morphogenesis *in vivo*

To determine whether hUCB-MSCs promote the anagen hair cycle, we injected hUCB-MSCs intra-dermally at multiple sites in depilated mouse dorsal skin. Saline injection and daily topical treatments of 3% minoxidil were used as controls. We determined the hair cycle stage by measuring the status of skin hair regrowth. We found that, by 5 weeks of treatment, hUCB-MSCs caused diffuse darkening of the dorsal skin, while the control groups showed no significant changes (data not shown). At 6 weeks of treatment, hair regrowth was complete in the hUCB-MSCs group, and the tip of the hair shaft emerged through the epidermis. Although the dorsal skin in the minoxidil-treated group had incomplete pigmentation and contained hairs in the early stage of the hair cycle, the dorsal skin of the normal and saline-injected groups retained large areas without anagen induction (Fig. 1A). After 6 weeks of treatment, we harvested the dorsal skin for histological analysis, which indicated that the hUCB-MSCs promoted the telogen-anagen transition (Fig. 1B). In particular, the hair follicles that were treated with hUCB-MSCs were transformed from the telogen phase to the early- and middle-anagen phases at 6 weeks (Fig. 1B). Remarkably, the hUCB-MSCs group prematurely reentered the anagen phase compared with the minoxidil-treated group (Fig. 1B). Furthermore, IHC data revealed that expression of the β-catenin protein, which is a positive regulator of hair growth, was up-regulated in the hUCB-MSCs group compared to the other groups (Fig. 1C).

To verify how hUCB-MSCs affect hair follicle morphogenesis, we implanted hUCB-MSCs (U) with epithelial stem cells (K) and dermal stem cells (D) of neonatal mice into nude mouse. Mixed U, K, and D exhibited increased hair follicle induction compared to the K plus D group (Figs. 1D and E). Interestingly, the K plus U group did not show hair follicle morphogenesis (Figs. 1D and E). Collectively, hUCB-MSCs enhanced hair follicle morphogenesis, represented as an increase of follicular neogenesis (Figs. 1D and E).

hUCB-MSCs increase cell viability and upregulate hair induction-related proteins in hDPCs

Changes in the microbiological environment cause hDPCs to lose their conduction ability to induce hair follicle formation in humans. To study the effects of hUCB-MSCs on the viability and characteristics of hDPCs, we estimated cell viability and ALP activity. The effect of hUCB-MSCs on hDPC proliferation and ALP activity was revealed using WST-8 and ALP-activity assays. hUCB-MSCs co-culture enhanced hDPC proliferation (Fig. 2A) and restored ALP activity, both of which are anagen markers of the hair cycle in hDPCs *in vitro* (Fig. 2B) [38].

We further examined AKT/GSK3β/β-catenin pathway regulation and proliferating cell nuclear antigen (PCNA) expression. Result revealed that protein expression of phosphorylated Akt (Ser473), phosphorylated GSK3β (Ser9), β-catenin, and PCNA was pronounced in the hDPCs plus hUCB-MSCs group compared to hDPCs only. These results indicate that β-catenin, AKT, and GSK3β, which are proteins contained in the pathway related to cell growth and proliferation, were up-regulated in hDPCs
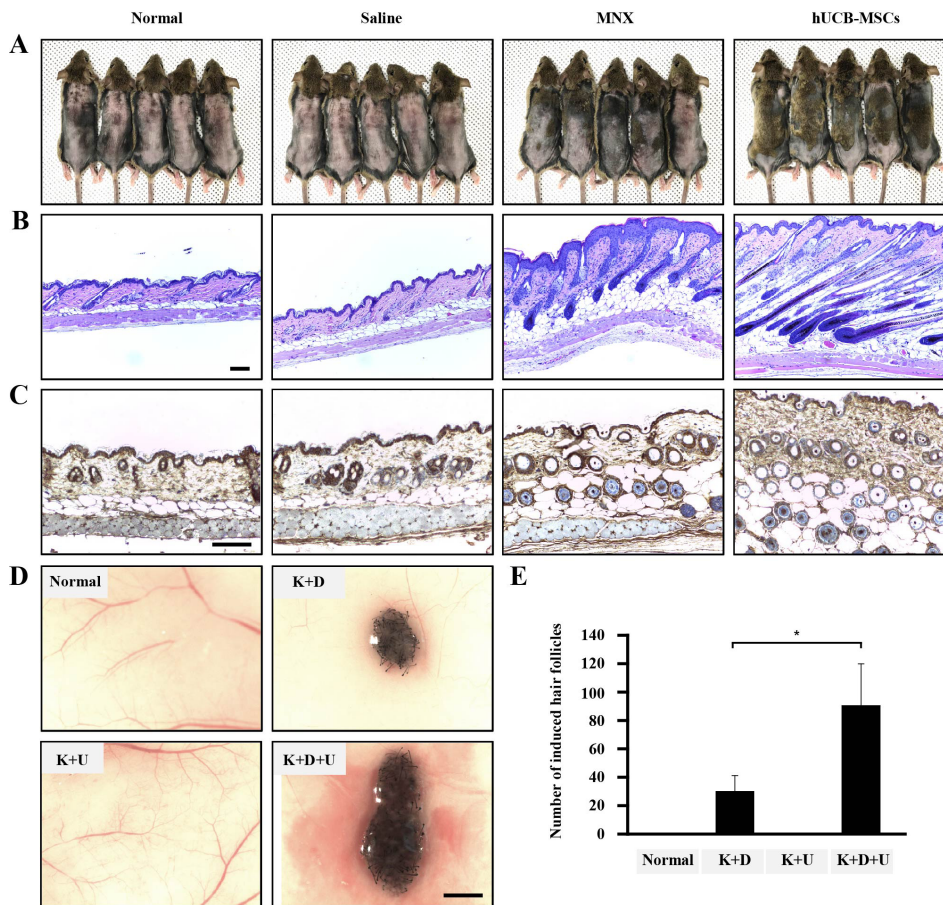
Fig. 1. The effects of hUCB-MSCs on induction of the hair cycle anagen stage in mice. The dorsal skin of six-week-old male C3H/HeJ mice was shaved and then injected with saline, treated with topical application of 3% minoxidil (MNX, 5 times per week), or injected with hUCB-MSCs (1×10^5 cells/head) (A) Gross images of hair regrowth in C3H/HeJ mice treated with either saline, MNX, or hUCB-MSCs at six weeks after shaving. (B) Histological analysis of dorsal skin samples from each group using H&E staining. Scale bar, 100 μm (C) Immunohistochemistry, dorsal skin samples from each group were stained with anti-β-catenin, Scale bar, 100 μm. (D) Patch assay: at 2 weeks, the nude mice were sacrificed, and newly generated hair follicles were counted. Scale bar, 1 mm. (E) Bar graph showing the number of each hair follicles as mean±SD. *p<0.05 *vs.* K plus D group. **p<0.01, ***p<0.001 *vs.* hDPCs alone.

by co-culture with hUCB-MSCs. We found that hUCB-MSCs not only promoted expression of hair anagen-induction-related proteins, but also upregulated the expression of PCNA in hDPCs (Figs. 2C and D). These findings suggest that, in hDPCs, the viability and ALP activity related to anagen conduction ability can be affected and repaired by hUCB-MSCs *in vitro*, and this effect is mainly regulated by AKT/GSK3β/β-catenin signaling.

Growth factor production in hDPC cultures with hUCB-MSCs

A screening of growth factor production was performed to discover the mechanisms underlying hair anagen induction by hUCB-MSCs. Culture media supernatants from hDPCs, hUCB-MSCs, and hDPCs plus hUCB-MSCs were collected after 5 days of culture and analyzed with an antibody array for 42 growth factors. Although several factors were detected in the hDPC plus hUCB-MSCs group, two growth factors were upregulated in the medium of the hDPC plus hUCB-MSCs group compared to the hDPC group (Figs. 3A and B). The hDPCs co-cultured in the presence of hUCB-MSCs showed a considerably increased levels of IGFBP-1 (about >1.25-fold) and VEGF (about >1.25-fold). Notably, IGFBP-1 was detected in the hUCB-MSCs-only group but less in the hDPC-only group. VEGF was also detected in the hUCB-

MSCs groups, but there was no significant difference compared to the hDPC-only group. In addition, secretion of IGFBP-2, -6, and PDGF-AA were detected both in the hDPCs and hDPCs plus hUCB-MSCs group, but there was no statistical significance to the increase. In conclusion, it was confirmed that the secretory source of IGFBP-1 is hUCB-MSCs.

The actions of IGFs are tightly modulated by a family of proteins called IGF-binding proteins (IGFBPs), of which IGFBP-1 to -6 have been characterized [39]. We measured IGF-1 and IGFBP-1 concentrations in culture media with an ELISA assay. Consistently, IGFBP-1 was not detected in the hDPCs alone, but the hUCB-MSCs and hDPC plus hUCB-MSCs group showed increased IGFBP-1 level compared to hDPCs alone (Fig. 3C). Additionally, VEGF concentration was detected in the hDPC alone group and hUCB-MSCs alone group, but it was overwhelmingly upward in the hDPC plus hUCB-MSCs compared to each alone group (Fig. 3D). These results suggest that the IGFBP-1 expression measured by the growth factor array is primarily secreted by the hUCB-MSCs, and this is related to VEGF concentration. In addition, we measured IGF-1 concentration in the culture media to determine the relationship between IGF-1 and IGFBP-1 expression. The protein concentration of IGF-1 was decreased in the hDPC plus hUCB-MSCs group compared to the hDPC group (Fig. 3E).
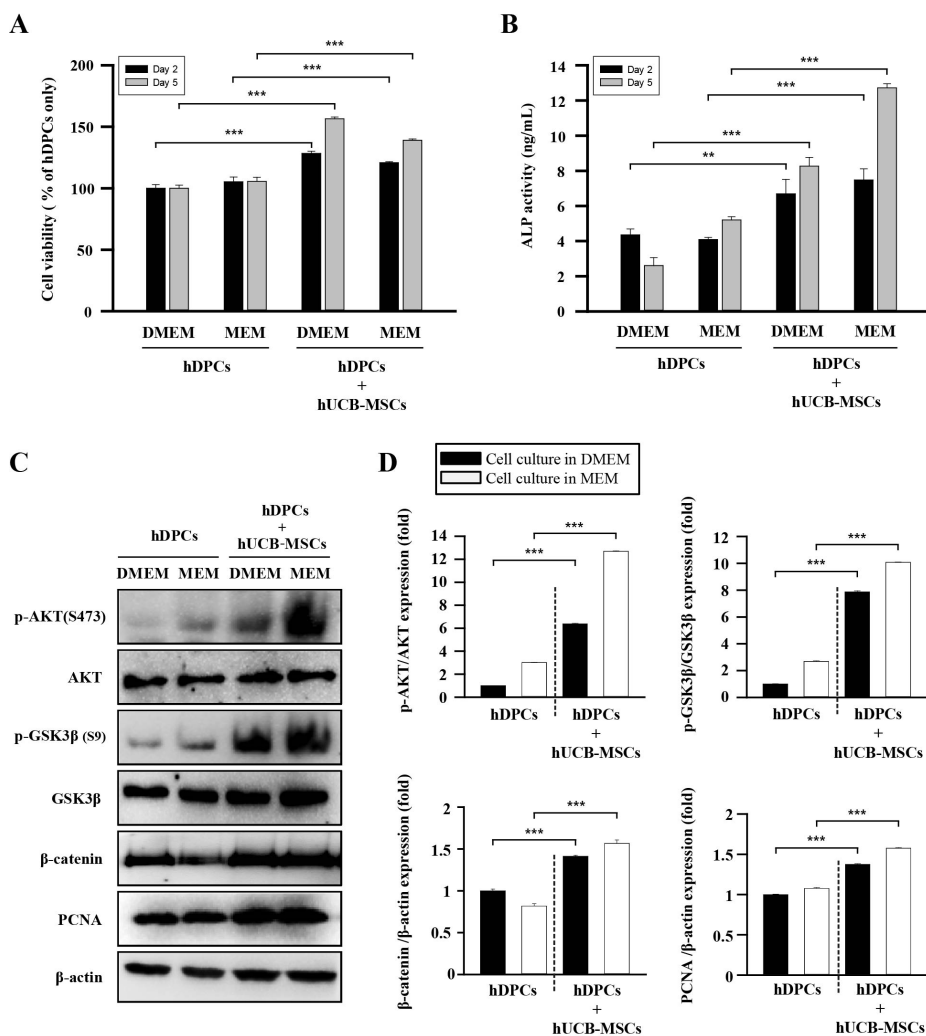
Fig. 2. The effects of hUCB-MSCs on cell viability, ALP activity, and AKT/GSK3β/β-catenin pathway regulation of hDPCs. hDPCs were co-cultured with hUCB-MSCs for 48 h or 120 h in two types of culture media (DMEM and MEM). (A) The cell viability was estimated using a WST-8 assay. (B) ALP activity. (C) Representative images of Western blot protein assays for p-AKT, AKT, p-GSK3β, GSK3β, β-catenin, and proliferating cell nuclear antigen (PCNA) in dermal papilla cells. hDPCs and hUCB-MSCs were seeded in 6-well transwell plates. After 48 h, the cell lysates were harvested for Western blot assays. (D) Intensities of the immunoreactive bands on the Western blots as quantified by densitometric analysis. For all graphs, the data is reported as mean±SD. *p<0.01, ***p<0.001 vs. hDPCs alone.

IGFBP-1 affects dermal papilla cell viability and promotes expression of diverse proteins related to hair induction

IGFBP-1, which was confirmed as the main component secreted by hUCB-MSCs, was studied to explore its independent function. To investigate the effects of IGFBP-1 on hDPCs, we treated hDPCs with recombinant human IGFBP-1 (rhIGFBP-1) protein and measured cell viability and VEGF secretion. The results indicated that the viability of hDPCs was significantly increased at 48 h after rhIGFBP-1 treatment (rhIGFBP-1 concentration: 12.5-200 ng/ml) (Fig. 4A). Furthermore, VEGF secretion also increased in an rhIGFBP-1 concentration-dependent manner in hDPCs (Fig. 4B). The expression of proteins related to hDPC conduction ability was confirmed by immunofluorescence in hDPCs. ALP and CD133 staining were strong after rhIGFBP-1 treatment (100 ng/ml) compared to the non-treatment group (rhIGFBP-1 (-)). Additionally, β-catenin expression and nuclear translocation were increased in the rhIGFBP-1 (+) group (Fig. 4C). Western blot data also revealed the upregulated protein expression of ALP, CD133, non-phosphorylation-β-catenin (non-p-β-catenin, activation

form), and β-catenin in the rhIGFBP-1 (+) group (Fig. 4D). To investigate the characteristics of hDPCs regarding the transformation to spheres and hair induction structures, the 3D sphere formation velocity of hDPCs was tested by seeding them in hanging-drop 96-well plates. When the seeding density exceeded 0.25×10^4 cells in the hanging-drop 96-well plate, the rapid aggregation of hDPC with a loose spheroid structure occurred on day 1, which then changed to a compact circular sphere after 5 days of incubation (Fig. 4E). The diameters of the spheres were quantified using phase contrast imaging on day 5. After seeding the hDPCs in hanging-drop 96-well plates, hDPCs treated with rhIGFBP-1 (100 ng/mL) produced spheres with an approximate diameter of 200 μm, which was larger than the sizes in the rhIGFBP-1 (-) group, at day 5. The maximum diameter of the rhIGFBP-1 (-) group was approximately half that of the rhIGFBP-1 (+) group (Figs. 4E and F). Collectively, these data support the idea that rhIGFBP-1 can stimulate cell proliferation; increase secretion of VEGF and enhance expression of ALP, CD133, and β-catenin; and promote the conduction ability to 3D tissue-like formation.
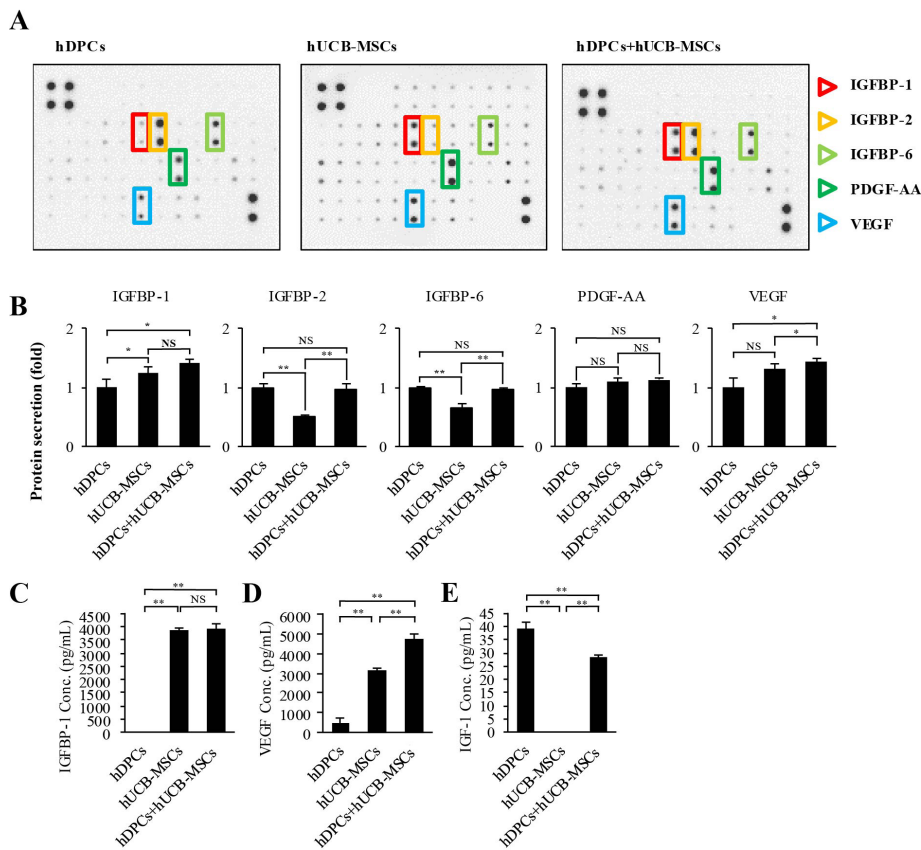
Fig. 3. Growth factor secretion profiles of hDPCs alone, hUCB-MSCs alone, and hDPCs plus hUCB-MSCs. (A) Representative images of the growth factor antibody array analysis in culture media obtained at 48 h of growth in each group. (B) Quantification of the cytokine array analysis of the culture media as the fold increase compared with hDPCs alone. The protein concentration in each culture media measured individual protein with ELISA. (C) IGFBP-1, (D) VEGF, and (E) IGF-1. Abbreviations are as follows: IGFBP-1, -2, and -6, insulin-like growth factor binding protein-1, -2, and -6; PDGF-AA, platelet-derived growth Factor-AA; VEGF, vascular endothelial growth factor; IGF-1, insulin-like growth factor-1. The data are reported as mean± SD. *p<0.05, **p<0.01, *vs.* hDPCs alone.

Effects of recombinant protein IGFBP-1 on co-localization of IGF-1 to dermal papilla cells

In previous reports, it was demonstrated that IGFBP-1 can act either directly or indirectly in biological environments [40] and form the complexes with IGF-1 [41]. We hypothesized that increased IGFBP-1 acts as a complex with IGF-1 in hDPCs. Therefore, we investigated the effects of rhIGFBP-1 treatment on the expression of IGF-1 in hDPCs. The results showed that most IGF-1 was co-localized with IGFBP-1, which was assumed to be the main secretory protein of hUCB-MSCs (Fig. 5). Interestingly, the protein expression of IGF-1 was slightly elevated in the rhIGFBP-1 (+) group compared to the rhIGFBP-1 (-) group (Fig. 5). These results suggest that secreted IGFBP-1 in hUCB-MSCs co-locate with IGF-1 and affects the expression of IGF-1 in hDPCs.

DISCUSSION

Alopecia is a serious dermatological disease that occurs due to diverse reasons [42]. Genetic factors and age have typically been considered the main causes of hair loss [43]. Androgenic alopecia results in decreased viability of dermal papilla cells and other cells comprising hair follicle tissue [16]. Dermal papilla cells play a central role in follicular growth and differentiation and direct hair

follicle cycling by secreting signaling factors to communicate to root sheath cells [44]. The hair follicle cycle is affected by androgen and several other factors produced by stressful environments, which cause a primary defect in hDPCs signaling, resulting in an inability to initiate the hair follicular anagen phase [45,46]. Therefore, the restoration of hDPCs hair induction ability has been considered a potential therapy for hair loss.

Mesenchymal stem cells (MSCs) exist as a heterogeneous population in animals and have great potential for use in tissue regeneration [47]. These MSCs are usually distinguished by their shape, small size, and high nuclear fluctuation, which determine their "stemness" and therapeutic capacity [48]. Attempts to regenerate tissue using biological factors secreted by UCB-MSCs have recently been reported [49,50]. In a previous study, implantation of BM-MSCs in normal and diabetic mice enhanced wound healing associated with increased angiogenesis [51]. In another study, mesenchymal stem cell transplantation has beneficial results due to its anti-inflammation potential in cardiac infarction damage [52]. In addition, intravenous injection of hUCB-MSCs has a role in the prevention of obesity as a mediator in macrophage polarization [53]. The effects of MSCs on tissue regeneration and anti-inflammatory effects have been verified, and the functions and main factors causing the therapeutic effects of MSCs have been widely explored [54]. In this study, hUCB-MSCs triggered hair anagen induction from the telogen phase *in vivo*. Furthermore,
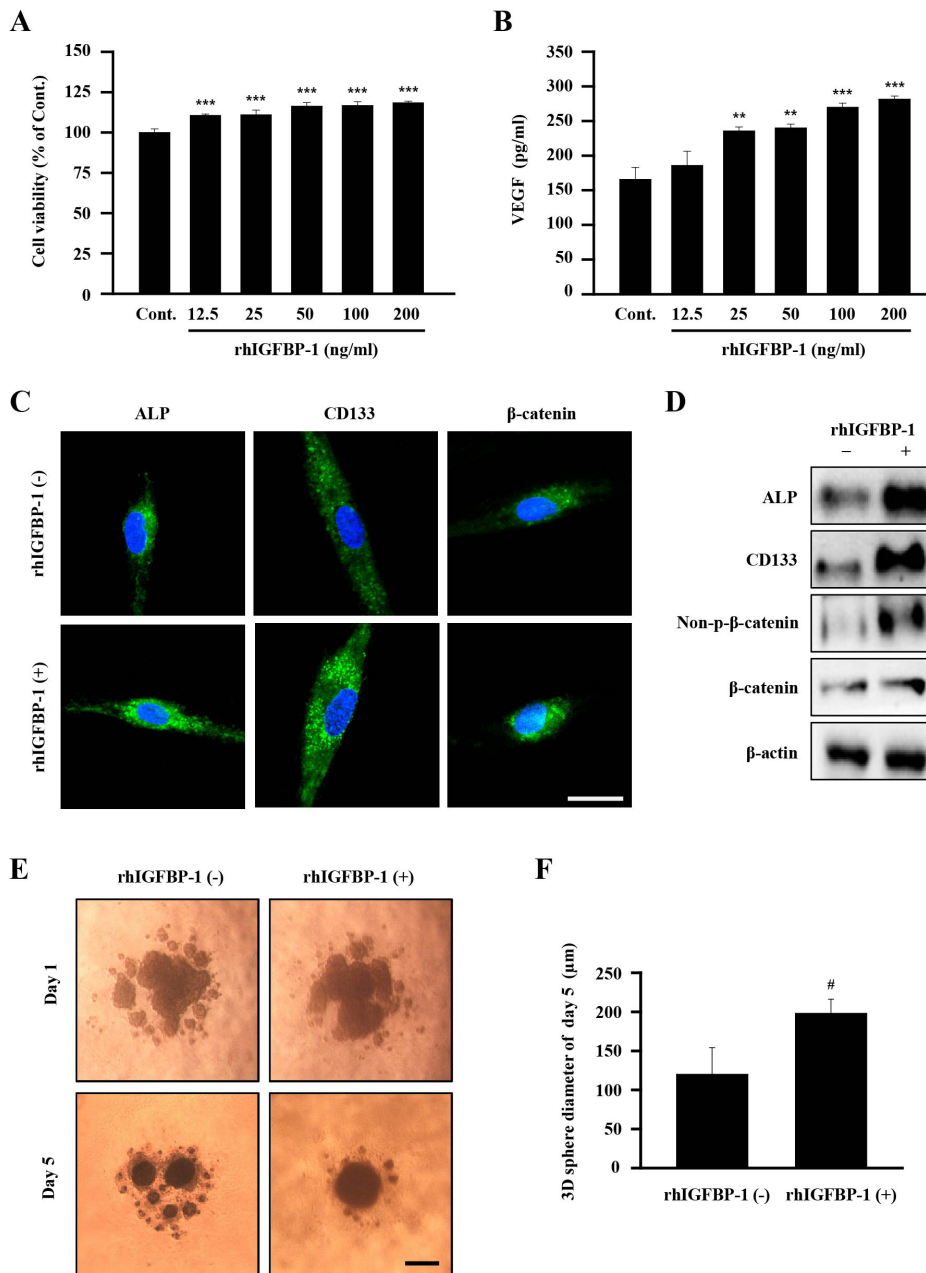
Fig. 4. The effects of recombinant IGFBP-1 on hDPC viability, VEGF secretion, expression of proteins related to hair anagen induction, and formation of 3D tissue-like structures of hDPCs. (A) Cell viability. Control hDPCs (Cont.) and IGFBP-1 (12.5-200 ng/ml)-treated hDPCs were cultured for 48 h, and the cell viability was measured using an WST-8 assay. (B) VEGF concentration in the culture media. Cont. and IGFBP-1 (12.5-200 ng/ml)-treated hDPCs were cultured for 48 h. The culture media was harvested, and VEGF concentration was measured using an ELISA assay. (C) Immunofluorescent staining of protein ALP, CD133, and β-catenin in hDPCs. rhIGFBP-1 (100 ng/ml) was administered to hDPCs (1×10^5) for 48 h. The cells were then stained to visualize the expression of anti-ALP, -CD133, and -β-catenin (Green). Scale bar 5 μm. (D) Representative images of Western blot. Cell lysates of hDPCs without or with rhIGFBP-1 (100 ng/mL) were immunoprobed with anti-ALP, -CD133, non-p-β-catenin, and β-catenin. Effect of rhIGFBP-1 (100 ng/mL) on the formation of hDPC spheroids after seeding for 5 days. (E) Representative images of passage 8-hDPCs from each treatment group (n=4) aggregated into microtissues in a regular manner (0.25×10^4 cells/well, scale bar 200 μm). (F) The bar graph shows the maximum tissue diameter produced in each group at Day 5. For all graphs, the data is shown as mean±SD. **p<0.01, ***p<0.001, *vs.* Cont. #p<0.01 *vs.* IGFBP (-).

hUCB-MSCs emphasized hair follicle morphogenesis, but in case of ablation of the neonatal dermal cell, hUCB-MSCs and epithelial cells did not undergo hair follicle generation. We assumed that hUCB-MSCs are not the main component of the newly generated hair follicle and may play a role in assisting dermal cells to conduct tissue generation. These findings indicate that hUCB-MSCs facilitate hair follicle regeneration and hair growth via a paracrine mechanism. In a previous report, MSC-conditioned medium that was modified to overexpress Wnt1a restored the hair cycle *in vivo* [34]. In another study, BM-MSCs increased angiogenesis in a diabetic mice wound model [51]. However, BM-MSCs were located adjacent to the vasculature rather than in the vascular walls [51]. This indicates that a paracrine effect of MSCs plays a

major role in angiogenesis and wound healing. In this study, we demonstrated that hDPCs co-cultured with hUCB-MSCs in a detached environment had increased cell viability and ALP activity and up-regulated the AKT/GSK3β/β-catenin pathway, indicating that paracrine factors have a major role in recruitments of hDPC conduction ability *in vitro*.

Insulin-like growth factor 1 (IGF-1) is an important growth factor in many biological environments [55,56]. In a previous report, it was found to have substantial structural homology with insulin and influence food intake and glucose metabolism in a similar manner to insulin [57]. Recently, IGF-1 has been suggested to play a crucial role in regulating cellular differentiation and tissue generation during the development of hair follicles [58].
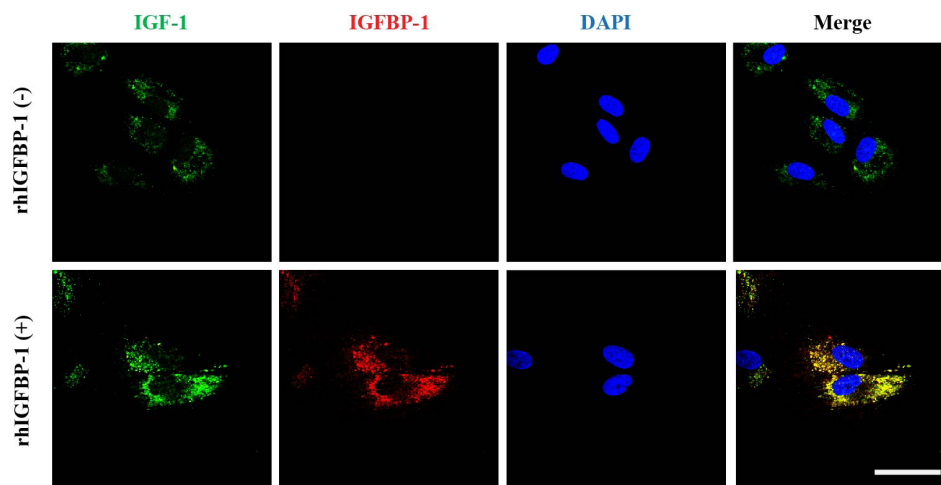
Fig. 5. The effects of recombinant IGFBP-1 on the expression of IGF-1 on hDPCs via the co-localization of an IGF-1 and IGFBP-1. hDPCs (1×10^5 cells) were treated with rhIGFBP-1 (100 ng/mL) for 48 h and then stained with anti-IGF-1 (green), anti-IGFBP-1 (red), and DAPI (nucleus, blue). Scale bar 20 μm.

To exert its physiological effects, IGF-1 activates cells by binding to specific cell-surface receptors [58]. In the circulatory system, this biological factor mediates the endocrine action of growth hormones on cellular growth and forms complexes with specific binding proteins (BPs) [41].

There are six insulin-like growth factor binding proteins (IGFBP-1~-6), which bind to IGF-1 and -2 with very high affinity [41]. Because their affinity to IGFBP is 2- to 50-fold greater than that of IGF-IR, these IGFBPs can modulate the distribution of IGF among the proteins in interstitial fluids [41]. In this study, we hypothesized that IGFBP-1 was be a major factor affecting dermal papilla cells. We assumed that, since IGF-1 protein is the autocrine factor of hDPCs bound to hDPCs with the assistance of IGFBP-1, its concentration in culture media was decreased compared to that of the non-assisted group (hDPCs alone).

Cells within hDPCs and dermal sheath (DS) are specially identified as mesenchymal cells and express distinct enzymes and molecules. Although the functions of most of these protein markers are not fully understood, they have been used to identify hDPCs and DS. The expression of some markers, like ALP and versican, correlates with hair inductive properties [59]. hDPCs easily lose their characteristics and conductivity *in vitro* in the absence of additional factors, such as WNT- or BMP-signaling [60]. In a previous report, beta-catenin was upregulated in hDPCs, resulting in increased expression of the mesenchymal stem cell marker CD133 [61]. Furthermore, this anagen-conductive protein is also increased during the formation of hDPCs 3D tissue-like aggregates *in vitro* and *in vivo* [62]. In this study, rhIGFBP-1 not only increased hDPCs viability and VEGF secretion, but also upregulated the protein expression of ALP, beta-catenin, and CD133. In addition, rhIGFBP-1 enhanced the formation velocity of 3D tissue-like aggregates of hDPCs *in vitro*. These results indicate that IGFBP-1 has a positive role in maintaining cell longevity and regulating the conduction ability of hair anagen momentum.

IGFBPs can affect cells directly or indirectly and modulate the function of IGF-1 in an endocrine, paracrine, or autocrine manner through IGF-1/IGFBP complexes [41]. In a previous report, when IGFBP-1 and IGF-1 were added to porcine aortic smooth muscle or human fibroblast cultures, the IGF-1/IGFBP-1 complex enhanced DNA synthesis compared to treatment with IGF-1 alone [41]. Additionally, IGFBP-1 allowed IGF-1 to remain in equilibrium with its high-affinity receptors for a prolonged interval [40,41]. In our results, rhIGFBP-1 formed a co-localization with IGF-1. Notably, this result suggests that the IGF-1/IGFBP-1 co-localization facilitates the interaction of IGF-1 with its receptor in hDPCs during the progression of the cell cycle.

In this study, we demonstrated that hUCB-MSCs can accelerate the initiation of the hair follicle telogen-anagen transition, increase the number of hairs *in vivo*, and enhance expression of proteins related to hair induction *in vitro*. Notably, IGFBP-1 (assumed as the main secretory factor of hUCB-MSCs) restores and promotes the hair-induction ability of hDPCs via an IGF-1/IGFBP-1 co-localization. Taken together, our findings indicate that hUCB-MSCs and their secretory protein IGFBP-1 can restore the ability of hDPCs to induce hair follicle regeneration, potentially providing alternative therapeutic methods for alopecia. In general, the immunosuppressive effect of the mesenchymal stem cell treatment is well known, as mentioned above. The occurrence of hair loss is also complex, and the immune response is one of its major causes. We would need to further investigate the effects of stem cell therapies on hair loss in a variety of biological environments.

ACKNOWLEDGEMENTS

CONFLICTS OF INTEREST

The authors declare no conflicts of interest.

REFERENCES

1. Ferriman D, Gallwey JD. Clinical assessment of body hair growth in women. *J Clin Endocrinol Metab.* 1961;21:1440-1447.
2. Harada T, Izaki S, Tsutsumi H, Kobayashi M, Kitamura K. Apoptosis of hair follicle cells in the second-degree burn wound unders hypernatremic conditions. *Burns.* 1998;24:464-469.
3. Leyden J, Dunlap F, Miller B, Winters P, Lebwohl M, Hecker D, Kraus S, Baldwin H, Shalita A, Draelos Z, Markou M, Thiboutot D, Rapaport M, Kang S, Kelly T, Pariser D, Webster G, Hordinsky M, Rietschel R, Katz HI, Terranella L, Best S, Round E, Waldstreicher J. Finasteride in the treatment of men with frontal male pattern hair loss. *J Am Acad Dermatol.* 1999;40:930-937.
4. Sinclair R. Male pattern androgenetic alopecia. *BMJ.* 1998;317:865-869.
5. Kligman AM. Pathologic dynamics of human hair loss. I. Telogen effuvium. *Arch Dermatol.* 1961;83:175-198.
6. Rogers NE, Avram MR. Medical treatments for male and female pattern hair loss. *J Am Acad Dermatol.* 2008;59:547-566.
7. Leavitt M, Perez-Meza D, Rao NA, Barusco M, Kaufman KD, Ziering C. Effects of finasteride (1 mg) on hair transplant. *Dermatol Surg.* 2005;31:1268-1276.
8. Rossi A, Cantisani C, Melis L, Iorio A, Scali E, Calvieri S. Minoxidil use in dermatology, side effects and recent patents. *Recent Pat Inflamm Allergy Drug Discov.* 2012;6:130-136.
9. Irwig MS, Kolukula S. Persistent sexual side effects of finasteride for male pattern hair loss. *J Sex Med.* 2011;8:1747-1753.
10. Olsen EA, Hordinsky M, Whiting D, Stough D, Hobbs S, Ellis ML, Wilson T, Rittmaster RS. The importance of dual 5alpha-reductase inhibition in the treatment of male pattern hair loss: results of a randomized placebo-controlled study of dutasteride versus finasteride. *J Am Acad Dermatol.* 2006;55:1014-1023.
11. Patwardhan N, Mysore V. Hair transplantation: standard guidelines of care. *Indian J Dermatol Venereol Leprol.* 2008;74 Suppl:S46-53.
12. Alonso L, Fuchs E. The hair cycle. *J Cell Sci.* 2006;119:391-393.
13. Chueh SC, Lin SJ, Chen CC, Lei M, Wang LM, Widelitz R, Hughes MW, Jiang TX, Chuong CM. Therapeutic strategy for hair regeneration: hair cycle activation, niche environment modulation, wound-induced follicle neogenesis, and stem cell engineering. *Expert Opin*

Biol Ther. 2013;13:377-391.
14. Harkey MR. Anatomy and physiology of hair. *Forensic Sci Int.* 1993;63:9-18.
15. Elliott K, Stephenson TJ, Messenger AG. Differences in hair follicle dermal papilla volume are due to extracellular matrix volume and cell number: implications for the control of hair follicle size and androgen responses. *J Invest Dermatol.* 1999;113:873-877.
16. Kwack MH, Sung YK, Chung EJ, Im SU, Ahn JS, Kim MK, Kim JC. Dihydrotestosterone-inducible dickkopf 1 from balding dermal papilla cells causes apoptosis in follicular keratinocytes. *J Invest Dermatol.* 2008;128:262-269.
17. Dallob AL, Sadick NS, Unger W, Lipert S, Geissler LA, Gregoire SL, Nguyen HH, Moore EC, Tanaka WK. The effect of finasteride, a 5 alpha-reductase inhibitor, on scalp skin testosterone and dihydrotestosterone concentrations in patients with male pattern baldness. *J Clin Endocrinol Metab.* 1994;79:703-706.
18. El-Badri NS, Hakki A, Saporta S, Liang X, Madhusodanan S, Willing AE, Sanberg CD, Sanberg PR. Cord blood mesenchymal stem cells: Potential use in neurological disorders. *Stem Cells Dev.* 2006;15:497-506.
19. Chung JY, Song M, Ha CW, Kim JA, Lee CH, Park YB. Comparison of articular cartilage repair with different hydrogel-human umbilical cord blood-derived mesenchymal stem cell composites in a rat model. *Stem Cell Res Ther.* 2014;5:39.
20. Kim JY, Kim DH, Kim JH, Yang YS, Oh W, Lee EH, Chang JW. Umbilical cord blood mesenchymal stem cells protect amyloid-β42 neurotoxicity via paracrine. *World J Stem Cells.* 2012;4:110-116.
21. Ng F, Boucher S, Koh S, Sastry KS, Chase L, Lakshmipathy U, Choong C, Yang Z, Vemuri MC, Rao MS, Tanavde V. PDGF, TGF-beta, and FGF signaling is important for differentiation and growth of mesenchymal stem cells (MSCs): transcriptional profiling can identify markers and signaling pathways important in differentiation of MSCs into adipogenic, chondrogenic, and osteogenic lineages. *Blood.* 2008;112:295-307.
22. Seo Y, Yang SR, Jee MK, Joo EK, Roh KH, Seo MS, Han TH, Lee SY, Ryu PD, Jung JW, Seo KW, Kang SK, Kang KS. Human umbilical cord blood-derived mesenchymal stem cells protect against neuronal cell death and ameliorate motor deficits in Niemann Pick type C1 mice. *Cell Transplant.* 2011;20:1033-1047.
23. Li XY, Zheng ZH, Li XY, Guo J, Zhang Y, Li H, Wang YW, Ren J, Wu ZB. Treatment of foot disease in patients with type 2 diabetes mellitus using human umbilical cord blood mesenchymal stem cells: response and correction of immunological anomalies. *Curr Pharm Des.* 2013;19:4893-4899.
24. Lee MJ, Yoon TG, Kang M, Kim HJ, Kang KS. Effect of subcutaneous treatment with human umbilical cord blood-derived multipotent stem cells on peripheral neuropathic pain in rats. *Korean J Physiol Pharmacol.* 2017;21:153-160.
25. Park HW, Kim Y, Chang JW, Yang YS, Oh W, Lee JM, Park HR, Kim DG, Paek SH. Effect of single and double administration of human umbilical cord blood-derived mesenchymal stem cells following focal cerebral ischemia in rats. *Exp Neurobiol.* 2017;26:55-65.
26. Yang SE, Ha CW, Jung M, Jin HJ, Lee M, Song H, Choi S, Oh W, Yang YS. Mesenchymal stem/progenitor cells developed in cultures from UC blood. *Cytotherapy.* 2004;6:476-486.
27. Olsen EA. Hair disorders. In: Irvine AD, Hoeger PH, Yan AC, editors. Harper's textbook of pediatric dermatology. Volume 1, 2, 3rd

ed. 2011. p.148.1-148.35.

28. Mounsey AL, Reed SW. Diagnosing and treating hair loss. *Am Fam Physician.* 2009;80:356-362.

29. Cotsarelis G, Millar SE. Towards a molecular understanding of hair loss and its treatment. *Trends Mol Med.* 2001;7:293-301.

30. Semenova E, Koegel H, Hasse S, Klatte JE, Slonimsky E, Bilbao D, Paus R, Werner S, Rosenthal N. Overexpression of mIGF-1 in keratinocytes improves wound healing and accelerates hair follicle formation and cycling in mice. *Am J Pathol.* 2008;173:1295-1310.

31. Leirós GJ, Attorresi AI, Balañá ME. Hair follicle stem cell differentiation is inhibited through cross-talk between Wnt/β-catenin and androgen signalling in dermal papilla cells from patients with androgenetic alopecia. *Br J Dermatol.* 2012;166:1035-1042.

32. Cardona-Gomez P, Perez M, Avila J, Garcia-Segura LM, Wandosell F. Estradiol inhibits GSK3 and regulates interaction of estrogen receptors, GSK3, and beta-catenin in the hippocampus. *Mol Cell Neurosci.* 2004;25:363-373.

33. Armstrong DD, Wong VL, Esser KA. Expression of beta-catenin is necessary for physiological growth of adult skeletal muscle. *Am J Physiol Cell Physiol.* 2006;291:C185-188.

34. Dong L, Hao H, Xia L, Liu J, Ti D, Tong C, Hou Q, Han Q, Zhao Y, Liu H, Fu X, Han W. Treatment of MSCs with Wnt1a-conditioned medium activates DP cells and promotes hair follicle regrowth. *Sci Rep.* 2014;4:5432.

35. Zheng Y, Du X, Wang W, Boucher M, Parimoo S, Stenn K. Organogenesis from dissociated cells: generation of mature cycling hair follicles from skin-derived cells. *J Invest Dermatol.* 2005;124:867-876.

36. Kang BM, Kwack MH, Kim MK, Kim JC, Sung YK. Sphere formation increases the ability of cultured human dermal papilla cells to induce hair follicles from mouse epidermal cells in a reconstitution assay. *J Invest Dermatol.* 2012;132:237-239.

37. Kwon TR, Oh CT, Choi EJ, Park HM, Han HJ, Ji HJ, Kim BJ. Human placental extract exerts hair growth-promoting effects through the GSK-3β signaling pathway in human dermal papilla cells. *Int J Mol Med.* 2015;36:1088-1096.

38. Iida M, Ihara S, Matsuzaki T. Hair cycle-dependent changes of alkaline phosphatase activity in the mesenchyme and epithelium in mouse vibrissal follicles. *Dev Growth Differ.* 2007;49:185-195.

39. Lin TC, Yen JM, Gong KB, Hsu TT, Chen LR. IGF-1/IGFBP-1 increases blastocyst formation and total blastocyst cell number in mouse embryo culture and facilitates the establishment of a stem-cell line. *BMC Cell Biol.* 2003;4:14.

40. Jones JI, Clemmons DR. Insulin-like growth factors and their binding proteins: biological actions. *Endocr Rev.* 1995;16:3-34.

41. Baxter RC. Insulin-like growth factor (IGF) binding proteins: the role of serum IGFBPs in regulating IGF availability. *Acta Paediatr Scand Suppl.* 1991;372:107-114.

42. Shapiro J, Madani S. Alopecia areata: diagnosis and management. *Int J Dermatol.* 1999;38 Suppl 1:19-24.

43. Rushton DH, Norris MJ, Dover R, Busuttil N. Causes of hair loss and the developments in hair rejuvenation. *Int J Cosmet Sci.* 2002;24:17-23.

44. Iguchi M, Hara M, Manome H, Kobayasi H, Tagami H, Aiba S. Communication network in the follicular papilla and connective tissue sheath through gap junctions in human hair follicles. *Exp Dermatol.* 2003;12:283-288.

45. Hibino T, Nishiyama T. Role of TGF-beta2 in the human hair

cycle. *J Dermatol Sci.* 2004;35:9-18.

46. Messenger AG. The control of hair growth: an overview. *J Invest Dermatol.* 1993;101(1 Suppl):4S-9S.

47. Phinney DG. Biochemical heterogeneity of mesenchymal stem cell populations: clues to their therapeutic efficacy. *Cell Cycle.* 2007;6:2884-2889.

48. Wagner W, Wein F, Seckinger A, Frankhauser M, Wirkner U, Krause U, Blake J, Schwager C, Eckstein V, Ansorge W, Ho AD. Comparative characteristics of mesenchymal stem cells from human bone marrow, adipose tissue, and umbilical cord blood. *Exp Hematol.* 2005;33:1402-1416.

49. Anderson DG, Markova D, An HS, Chee A, Enomoto-Iwamoto M, Markov V, Saitta B, Shi P, Gupta C, Zhang Y. Human umbilical cord blood-derived mesenchymal stem cells in the cultured rabbit intervertebral disc: a novel cell source for disc repair. *Am J Phys Med Rehabil.* 2013;92:420-429.

50. Liu GP, Li YL, Sun J, Cui L, Zhang WJ, Cao YL. Repair of calvarial defects with human umbilical cord blood derived mesenchymal stem cells and demineralized bone matrix in athymic rats. *Zhonghua Zheng Xing Wai Ke Za Zhi.* 2010;26:34-38.

51. Chen L, Tredget EE, Wu PY, Wu Y. Paracrine factors of mesenchymal stem cells recruit macrophages and endothelial lineage cells and enhance wound healing. *PLoS One.* 2008;3:e1886.

52. Guo J, Lin GS, Bao CY, Hu ZM, Hu MY. Anti-inflammation role for mesenchymal stem cells transplantation in myocardial infarction. *Inflammation.* 2007;30:97-104.

53. Xie Z, Hao H, Tong C, Cheng Y, Liu J, Pang Y, Si Y, Guo Y, Zang L, Mu Y, Han W. Human umbilical cord-derived mesenchymal stem cells elicit macrophages into an anti-inflammatory phenotype to alleviate insulin resistance in type 2 diabetic rats. *Stem Cells.* 2016;34:627-639.

54. Arthur A, Zannettino A, Gronthos S. The therapeutic applications of multipotential mesenchymal/stromal stem cells in skeletal tissue repair. *J Cell Physiol.* 2009;218:237-245.

55. Davis ME, Hsieh PC, Takahashi T, Song Q, Zhang S, Kamm RD, Grodzinsky AJ, Anversa P, Lee RT. Local myocardial insulin-like growth factor 1 (IGF-1) delivery with biotinylated peptide nanofibers improves cell therapy for myocardial infarction. *Proc Natl Acad Sci U S A.* 2006;103:8155-8160.

56. Sukhanov S, Higashi Y, Shai SY, Vaughn C, Mohler J, Li Y, Song YH, Titterington J, Delafontaine P. IGF-1 reduces inflammatory responses, suppresses oxidative stress, and decreases atherosclerosis progression in ApoE-deficient mice. *Arterioscler Thromb Vasc Biol.* 2007;27:2684-2690.

57. Nam SY, Lee EJ, Kim KR, Cha BS, Song YD, Lim SK, Lee HC, Huh KB. Effect of obesity on total and free insulin-like growth factor (IGF)-1, and their relationship to IGF-binding protein (BP)-1, IGFBP-2, IGFBP-3, insulin, and growth hormone. *Int J Obes Relat Metab Disord.* 1997;21:355-359.

58. Weger N, Schlake T. Igf-I signalling controls the hair growth cycle and the differentiation of hair shafts. *J Invest Dermatol.* 2005;125:873-882.

59. Toyoshima KE, Asakawa K, Ishibashi N, Toki H, Ogawa M, Hasegawa T, Irié T, Tachikawa T, Sato A, Takeda A, Tsuji T. Fully functional hair follicle regeneration through the rearrangement of stem cells and their niches. *Nat Commun.* 2012;3:784.

60. Rendl M, Polak L, Fuchs E. BMP signaling in dermal papilla cells

is required for their hair follicle-inductive properties. *Genes Dev.* 2008;22:543-557.

61. Zhou L, Yang K, Xu M, Andl T, Millar SE, Boyce S, Zhang Y. Activating β-catenin signaling in CD133-positive dermal papilla cells increases hair inductivity. *FEBS J.* 2016;283:2823-2835.

62. Huang CF, Chang YJ, Hsueh YY, Huang CW, Wang DH, Huang TC, Wu YT, Su FC, Hughes M, Chuong CM, Wu CC. Assembling composite dermal papilla spheres with adipose-derived stem cells to enhance hair follicle induction. *Sci Rep.* 2016;6:26436.